Biophysical Journal Volume 70 April 1996 1662–1668

Potassium Current Inhibition by Nonselective Cation Channel-Mediated Sodium Entry in Rat Pheochromocytoma (PC-12) Cells

Carsten Strübing* and Jürgen Hescheler‡
*Institut für Pharmakologie, Universitätsklinikum Benjamin Franklin, Freie Universität Berlin, D-14195 Berlin, and ‡Institut für Neurophysiologie der Universität zu Köln, D-50931 Köln, Germany

ABSTRACT Under physiological conditions, nonselective cation (NSC) channels mediate the entry of cations into cells, the most important being Na^+ and Ca^{2+}. In contrast to the Ca^{2+}-dependent signaling mechanisms, little is known about the consequences and the spatial distribution of intracellular [Na^+] elevation. In this study we demonstrate that Na^+ entry, during the opening of ATP-activated NSC channels, leads to an inhibition of voltage-dependent K^+ currents (I_K) in cromaffin-like undifferentiated PC-12 cells. The effect was dependent on the charge carrier as well as on the density of the ATP-activated current. Extracellular alkali cations (Na^+, Li^+) were more efficient than NH_4^+ in suppressing I_K. Intracellular infusion of Na^+ had the same effect as Na^+ influx through ATP-activated NSC channels. The inhibition of I_K persisted when the total ATP-induced Na^+ entry was reduced by membrane depolarization, suggesting a spatial restriction of the required Na^+ accumulation. Our results indicate that NSC channels influence the function of other ion channels by changing local intracellular ion concentrations.

INTRODUCTION

Nonselective cation (NSC) channels constitute a heterogeneous class of ion channels including receptor-operated, cyclic nucleotide-activated channels and channels gated upon emptying of Ca^{2+} stores (Hescheler and Schultz, 1993). In contrast to the ion-selective channels, NSC channels do not discriminate between cations, leading to more drastic changes of intracellular cation homeostasis.

Previous studies concentrated on the NSC channel-mediated rise of intracellular Ca^{2+}, which is established as a second messenger activating common signaling pathways such as protein phosphorylation (Schulman, 1993) and gene transcription (Roche and Prentki, 1994). Ca^{2+} has also been determined to directly and locally modulate ion channel functions (Gola and Crest, 1993; Imredy and Yue, 1992). Much less is known about the effects and the spatial distribution of $[Na^+]_i$ increases. The influx of Na^+ is mainly considered to be a depolarizing force causing excitation and Ca^{2+} entry via voltage-operated Ca^{2+} channels. However, recent studies demonstrated an inhibition of voltage-dependent ion channels after NSC channel (AMPA/kainate receptor) activation in murine glial cells, possibly induced by Na^+ influx (Borges et al., 1994; Jabs et al., 1994). This led us to study in more detail the consequences of Na^+ influx and accumulation during NSC channel activation.

Rat pheochromocytoma cells of the line PC-12 are a suitable model for investigating the influence of cation currents through ATP-activated NSC channels (I_{ATP}) on voltage-dependent K^+ currents (I_K). The electrophysiological properties of I_{ATP} exhibiting the pharmacological profile of P_{2x} receptors (Kim and Rabin, 1994; Brake et al., 1994) have been extensively studied (Inoue et al., 1989; Nakazawa et al., 1990; Nakazawa and Hess, 1993). I_K in undifferentiated PC-12 cells was described by Hoshi and Aldrich (1988a). Four different types of voltage-dependent K^+ channels (denoted K_w, K_x, K_y, and K_z) were identified on the single-channel level (Hoshi and Aldrich, 1988a,b).

In this study, we demonstrate that activation of I_{ATP} is accompanied by a strong inhibition of I_K. We provide evidence that Na^+ entry through the ATP-activated NSC channels and an accumulation of Na^+ in the vicinity of the plasma membrane induce this effect. Local changes of $[Na^+]_i$ may represent a general aspect of NSC channel function regulating other ion channels and membrane proteins.

MATERIALS AND METHODS

Cell culture and electrophysiology

PC-12 cells (CRL-1721; ATCC, Rockville, MD) were grown as previously described (Gollasch et al., 1991). Cells were transferred into a perfusion chamber (4 ml/min), and whole-cell patch-clamp experiments (Hamill et al., 1981) were performed at 37°C. Patch pipettes with resistances between 3 and 6 MΩ in standard external solution were prepared from borosilicate glass capillaries (Jencons, Leight Buzzard, England). Currents were recorded using an EPC 7 patch-clamp amplifier (List Electronics, Darmstadt, Germany) and a CED (Cambridge Electronic Design, Cambridge, England) interface. Off-line data analysis was performed with the CED software and SigmaPlot 5.0 (Jandel Corp., Corte Madera, CA). Statistical values are given as means ± SD. Capacitance cancellation and series resistance compensation (50–70%) of the EPC 7 were routinely used. The cellular surfaces were calculated from membrane capacitances (assuming a specific capacitance of 1 $\mu F/cm^2$) determined during 2-ms voltage ramp pulses from −80 to −100 mV. The patch pipettes were filled with a high K^+ solution containing (in mM): K_4-1,2-bis(2-aminophenoxy)ethane-*N,N,N',N'*-tetraacetic acid (K_4-BAPTA) 20, KCl 50, $MgCl_2$ 1, Mg_2-ATP 3, HEPES 10 (pH adjusted to 7.4 with KOH at 37°C). The

Received for publication 27 March 1995 and in final form 3 January 1996.

Address reprint requests to Dr. J. Hescheler, Institut für Neurophysiologie, Universität zu Köln, Robert-Koch-Strasse 39, D-50931 Köln, Germany. Tel.: 49-0221-478-6960; Fax: 49-0221-478-6965; E-mail: hescheler@neuro.physiologie.uni-koeln.de.

0006-3495/96/04/1662/07 $2.00

resulting free Mg^{2+} concentration was 2.3 mM, as calculated with the software of Schubert (1990).

In some experiments guanosine-5′-*O*-(2-thiodiphosphate) or cAMP was added to the solution. For intracellular infusion of Na^+, the high K^+ solution was mixed in different ratios with a high Na^+ solution containing (in mM): NaCl 135, $MgCl_2$ 1, Mg_2-ATP 3, HEPES 10, BAPTA 20 (pH adjusted to 7.4 with NaOH at 37°C). The internal solution for infusion of *N*-methyl-D-glucamine (NMDG) contained (in mM): NMDG 65, KCl 65, $MgCl_2$ 1, Mg_2-ATP 3, HEPES 10, BAPTA 20 (pH adjusted to 7.4 with HCl at 37°C). The standard external solution contained (in mM): NaCl 140, KCl 5.4, $CaCl_2$ 1.8, $MgCl_2$ 1, glucose 10, HEPES 10 (pH adjusted to 7.4 with NaOH at 37°C). All chemicals were purchased from Sigma (Deisenhofen, Germany).

RESULTS

Depolarizing voltage pulses to potentials positive to −20 mV activated I_K as described by Hoshi and Aldrich (1988a) (Fig. 1). Simultaneous superfusion of PC-12 cells with 20 μM ATP induced an additional inward-rectifying current I_{ATP} (Nakazawa et al., 1990), which was associated with an inhibition of I_K (Fig. 1). Both the activation of I_{ATP} and the inhibition of I_K were readily reversible after removal of ATP. The whole-cell *I-V* relation was constructed from the peak current responses to voltage pulses with test potentials varying between −100 and 100 mV (Fig. 1 B). The *I-V* relations were nearly identical to the currents in response to linear voltage ramps (from −100 to 100 mV, slope 2 V/s, 0.33 Hz, in the following denoted as "standard protocol") (Fig. 1 *B*), making it easier to quickly characterize the whole-cell *I-V* relation by applying the voltage ramp protocol. Under this condition, the mean I_K amplitude at 80 mV amounted to 1372 ± 739 pA (n = 58).

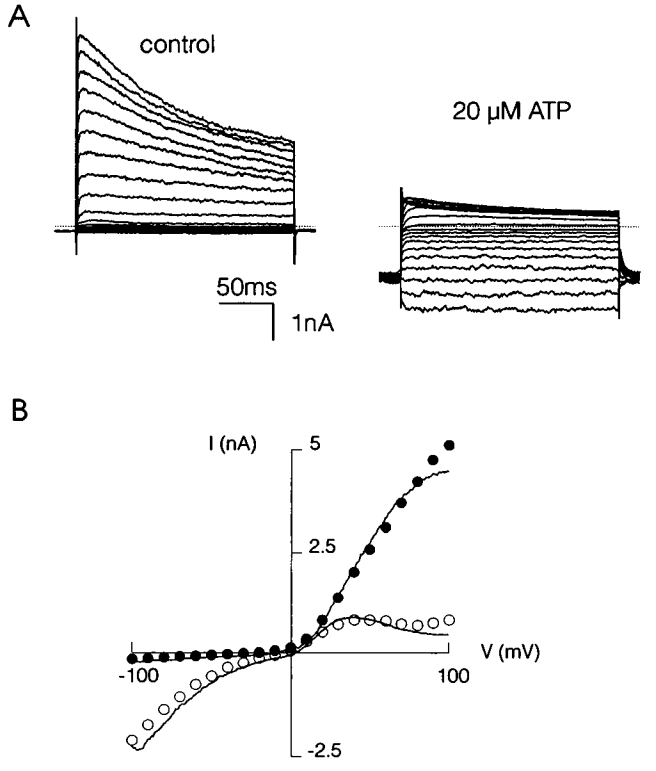

FIGURE 1 Effect of ATP on I_K in undifferentiated PC-12 cells. (*A*) I_K was measured during 200-ms rectangular voltage clamp pulses from a holding potential of −80 mV to test potentials ranging from −100 to 100 mV (10-mV increments). Original current traces before (*left*) and after (*right*) 20 s in the presence of ATP are shown. The dashed line indicates the zero current level. (*B*) *I-V* curves were constructed from traces shown in *A* by plotting peak current amplitudes before (●) and after (○) application of ATP versus the test potential. The superimposed current traces were measured on the same cell using the standard protocol (200-ms voltage ramps from −100 to 100 mV were applied with 0.33 Hz from a holding potential of −80 mV) before and after application of ATP (A and B from cell c2706bk).

To separate the contribution of I_{ATP} and I_K to the total whole-cell current we used the K^+ channel blocker quinidine, which was previously reported to completely and reversibly inhibit I_K in PC-12 cells (Hoshi and Aldrich, 1988a). Fig. 2 shows that there was no detectable quinidine-sensitive current in the voltage range between −20 and −100 mV. Likewise, I_{ATP} measured after blockage of I_K by quinidine was characterized by a strong inward rectification. This shows that I_{ATP} does not contribute to the whole-cell current at potentials more positive than −20 mV. Therefore, the voltage dependencies of I_K and I_{ATP} allow both components to be determined separately at 80 and −80 mV, respectively. The experiment also shows that the observed decrease of the outward current during ATP application is not due to a superposition of I_K and I_{ATP} but to an inhibition of I_K.

Voltage-dependent Ca^{2+} currents were not blocked, because their amplitudes were negligibly small and the removal of extracellular Ca^{2+} did not alter the observed effects (see below).

The time course of I_{ATP} (at −80 mV; Fig. 3, *open squares*) and I_K (at 80 mV; *filled squares*) during superfusion of PC-12 cells by 20 μM ATP was measured under repetitive standard protocol ramp pulses (Fig. 3). After application of ATP, I_{ATP} activated within approximately 3–6 s and slowly desensitized thereafter. The decrease of I_K took place within 15 ± 5.4 s (n = 40, range 9–21 s), and a delayed recovery of I_K after removal of ATP was observed. Even after complete deactivation of I_{ATP}, the inhibition of

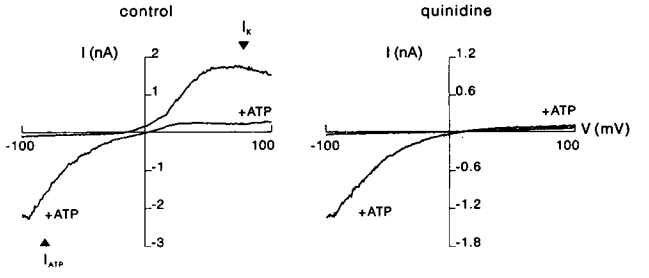

FIGURE 2 Separation and determination of I_{ATP} and I_K from the total whole-cell current. The whole-cell *I-V* relation of a PC-12 cell was measured under control conditions (*left*) and after (*right*) inhibition of I_K with 500 μM quinidine. ATP (20 μM) alone (*left*) or in the presence of quinidine (*right*) induced a strongly inward-rectifying I_{ATP} without a noticeable outward component (*right*). I_{ATP} and I_K were subsequently determined at −80 or 80 mV respectively, indicated by the arrowheads (cell c2206bq).

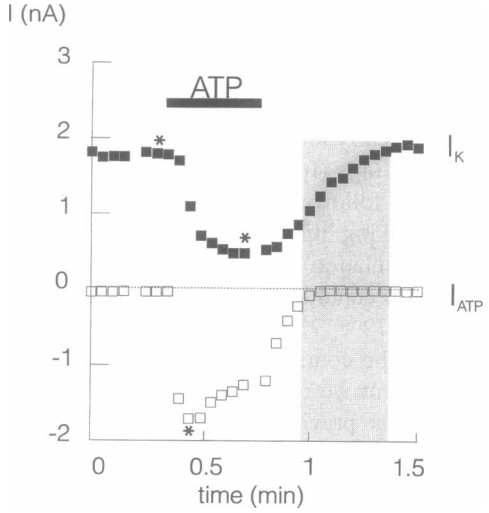

FIGURE 3 Time course of I_{ATP} and the accompanying inhibition of I_K. The time course of I_K (■) and I_{ATP} (□) was recorded simultaneously using the standard protocol. I_K and I_{ATP} were measured at 80 and −80 mV, respectively, and plotted versus time. The application of 20 μM ATP is indicated by the bar. The asterisks mark the values used to determine I_K inhibition and I_{ATP}. The gray area shows the delay of recovery from I_K inhibition after complete deactivation of I_{ATP} (cell c0504as).

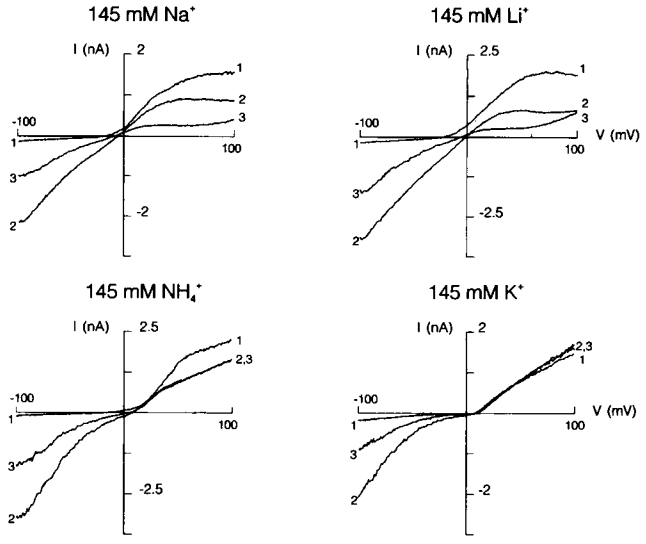

FIGURE 4 Dependence of I_K inhibition on the extracellular charge carrier of I_{ATP}. Currents were measured using the standard protocol before and during application of 20 μM ATP. The extracellular solutions were nominally without divalent cations and contained (in mM): X^+ 145, glucose 10, HEPES 10 (pH adjusted to 7.4 with KOH at 37°C). X^+ is given above each panel. Shown are control traces (*1*), traces at maximum activation of I_{ATP} (*2*), and traces at maximum inhibition of I_K (*3*). For a better comparison, cells of similar size were selected (cells c2004ab, c2004ae, c1005aq, and c0606ae).

I_K persisted for 10–20 s. For comparison of multiple similar experiments, we determined the activation of I_{ATP} and inhibition of I_K at the times of maximum effects (indicated by the asterisks in Fig. 3). The mean I_{ATP} amplitude amounted to 770 ± 781 pA (n = 52), and I_K inhibition was 55 ± 24% (n = 52).

The delayed response of I_K compared to I_{ATP} could be due to i) a coupling of ATP receptors to K^+ channels via a slow signaling transduction cascade or ii) an indirect blockage of I_K by I_{ATP}-induced intracellular ion concentration changes. Both alternatives were investigated.

Pretreatment of PC-12 cells with the broad-range protein kinase inhibitor staurosporin (10 μM for 1 h, n = 3) or infusion of 100 μM cAMP (n = 4) via the patch pipette did not noticeably change inhibition of I_K. Furthermore, preincubation of cells for 24 h with both cholera (2 μg/ml) and pertussis (100 ng/ml) toxin did not influence I_K inhibition (49.2 ± 23%, n = 9), in comparision to I_K inhibition in control cells from the same experimental series (46.3 ± 22.7%, n = 8, t-test). To exclude a signal transduction by cholera and pertussis toxin-insensitive guanine nucleotide-binding proteins (G-proteins), we intracellularly infused 1 mM guanosine-5′-*O*-(2-thiodiphosphate) (n = 6), which was also ineffective in modulating the inhibition of I_K.

A blockage of I_K via Ca^{2+}-activated signaling pathways is unlikely as well, because we employed a strong intracellular Ca^{2+} buffer (20 mM BAPTA). Moreover, removal of extracellular Ca^{2+} did not influence I_K inhibition (Fig. 4).

To test the second alternative, ATP-induced inhibition of I_K was studied with various monovalent charge carriers of I_{ATP} (Fig. 4). Li^+ but not NH_4^+ or K^+ fully substituted for Na^+. NH_4^+ induced a significantly smaller inhibition of I_K than Na^+ in the same cells ($p < 0.01$, n = 5, t-test). With K^+ as the only external monovalent cation, ATP activated I_{ATP} in a manner similar to that of Na^+ but did influence I_K (Fig. 4). Only with Na^+ and Li^+ but not with NH_4^+ as charge carrier of I_{ATP} did the inhibited I_K show a typical *I-V* relation characterized by a negative slope at potentials between 50 and 80 mV (Fig. 4; see also Fig. 1 *B*).

The different densities of P_{2x} receptors in the various PC-12 cells measured provide a possibility of correlating different cation influxes during application of ATP with the inhibition of I_K. In Fig. 5 the inhibition of I_K in each cell is given in relation to the amount of charge entry. I_K inhibition was positively correlated to the charge entry, with a maximum inhibition of more than 85% occurring at integral influxes larger than 20 pC/μm^2. The dependency of I_K inhibition on the integral charge entry is best approximated by a monoexponential curve (Fig. 5).

For a nonselective cation channel like the P_{2x} receptor, the inward current integral is not equal to the net Na^+ entry. Assuming a simple electrodiffusion through a homogeneous pore, the Goldman-Hodgkin-Katz (GHK) equation (Hodgkin, 1951) can be used to determine the relative current fraction (I_x) carried by the ion species X if the relative permeabilities (p_x) of all ions are known:

$$I_x(V) = p_x z_x^2 \frac{VF^2}{RT} \frac{[X]_i - [X]_o \exp(-z_x FV/RT)}{1 - \exp(-z_x FV/RT)} \quad (1)$$

and

$$i_x(V) = \frac{I_x(V)}{\sum I_x(V)}, \quad (2)$$

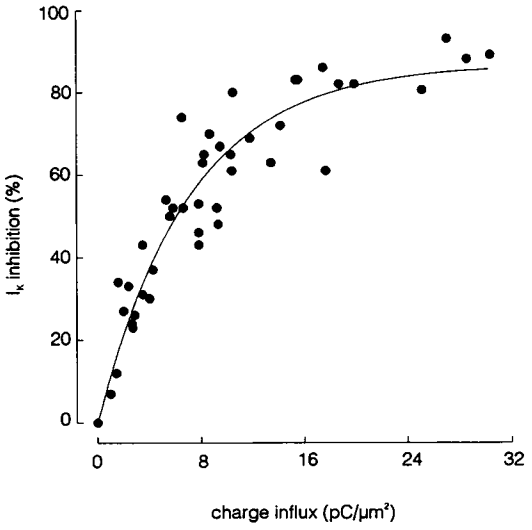

FIGURE 5 Dependence of I_K inhibition on charge influx in undifferentiated PC-12 cells. The relative I_K inhibition was determined at 80 mV as the ratio between control I_K and steady-state I_K in the presence of 20 μM ATP. The inhibition of I_K was plotted versus the inward current integral measured from the application of ATP until a constant I_K inhibition was observed. The integral influx was normalized to the cell size (expressed by the membrane surface), and the data points were fitted by a monoexponential function: $y = 86.7 * (1 - \exp(-0.14 * x))$ (*solid line*).

where $[X]_i$ and $[X]_o$ are the intra- and extracellular activities and $I_X(V)$ is the current carried by the ion species X; V is the membrane potential and z_x is the valency of ion X. RT and F have their usual meanings. If any anion permeability is neglected, fluxes of Na^+, K^+, Ca^{2+}, and Mg^{2+} contribute to the measured I_{ATP}. Therefore, the maximum current $I(V)$ activated by ATP is

$$I(V) = \sum I_x(V) = I_{Na}(V) + I_K(V) + I_{Ca}(V) + I_{Mg}(V). \quad (3)$$

From Eqs. 1 and 3 and assuming relative permeabilities of the contributing cations reported in the literature (Nakazawa et al., 1990; Benham and Tsien, 1987), we calculated $I_{Na}(V)$ and $I(V)$ (Fig. 6 *A*). Although the calculated reversal potential (V_{rev} = 20.5 mV) is in good agreement with the experimental value of 18 ± 4 mV (n = 3) measured after blockage of I_K with quinidine (see Fig. 2), it is clear that $I(V)$ does not adequately describe the inward rectifying I-V relation of I_{ATP} (Fig. 2).

To account for this property of I_{ATP}, we used a slightly modified formula originally introduced by Hagiwara and Takahashi to describe the intrinsic voltage dependence of inward rectifier K^+ channels (Hagiwara and Takahashi, 1974; Hille and Schwarz, 1978; see also Sands and Barish, 1992, for the nonselective nAChR (nicotinic acetylcholine receptor)):

$$I_{ATP}(V) = \frac{I(V)}{\exp(z'F/RT(V - V_H - V_{rev}) + 1}, \quad (4)$$

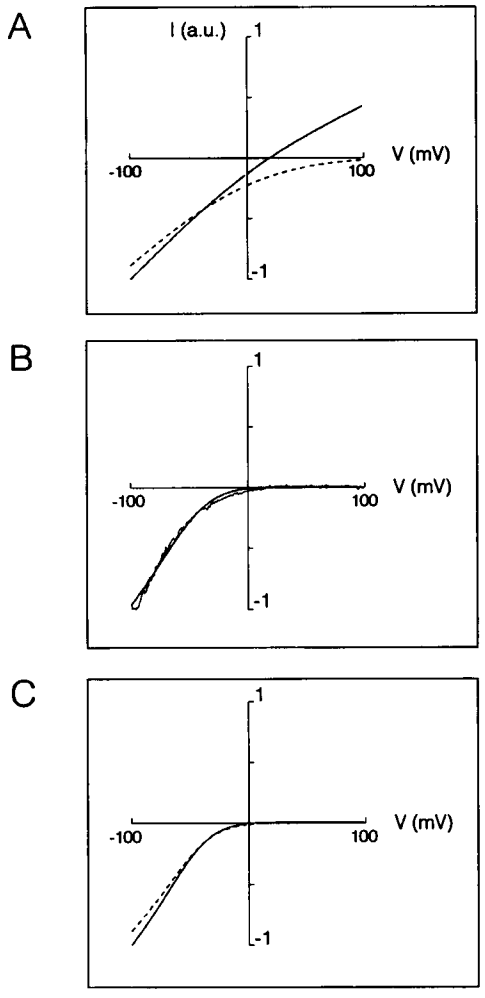

FIGURE 6 Relative contribution of Na^+ to the ATP-induced charge entry. (*A*) The maximum cation current ($I(V)$; *solid line*) and the fraction carried by Na^+ ($I_{Na}(V)$; *dashed line*) were calculated according to Eqs. 1 and 3 with $p_{Na}/p_K/p_{Ca}/p_{Mg}$ = 1/0.5/5.4/1.6. $[Na^+]_i$ and $[Ca^{2+}]_i$ were estimated as 1 μM and 1 nM, respectively. The activity coefficients of monovalent and divalent ions were taken as 0.75 and 0.3, respectively (Benham and Tsien, 1987). (*B*) Average I_{ATP} in the presence of 500 μM quinidine (n = 3), normalized to the minimum current. The solid line represents the best fit of the experimental data to Eq. 4, yielding z' = 1.39 and V_H = −69 mV. (*C*) The parameters obtained in *B* were used to calculate $I_{ATP}(V)$ (*solid line*) with Eq. 4. The current carried by Na^+ ($I_{ATP,Na}(V)$; *dashed line*) was calculated with Eq. 5.

where the parameter z' can be interpreted in terms of a Boltzmann relation as the effective valency of a blocking particle and V_H as the potential where half of the channels are blocked. V_{rev} is the reversal potential. Fig. 6 *B* shows that I_{ATP} could be well fitted using Eq. 4. Assuming that the relative permeabilities are voltage independent, the fraction of I_{ATP} carried by Na^+ is

$$I_{ATP,Na}(V) = I_{ATP}(V) * i_{Na}(V). \quad (5)$$

The functions $I_{ATP,Na^+}(V)$ and $I_{ATP}(V)$ (Fig. 6 *C*) allow the Na^+ influx to be estimated for each cell from the experimental values obtained for I_{ATP} at −80 mV. Equation 5

predicts that about 90% of the total charge entry at the holding potential, usually set to −80 mV, as well as during the voltage ramp pulses, was carried by Na^+. At positive potentials there should be no considerable Na^+ influx.

Our standard voltage clamp conditions (holding potential −80 mV) caused a nonphysiologically high entry of Na^+. Consequently, we employed an alternative voltage clamp protocol to reduce the Na^+ influx. The cells were held close to the reversal potential of I_{ATP} at 10 mV or 30 mV, where according to Eq. 5 the Na^+ influx is only 1.2% or 0.4%, respectively, of that at −80 mV. A considerable entry of Na^+ was only allowed during short prepulses to −80 mV and the negative part of the test ramp pulses during which I_K was determined (Fig. 7 A). This "prepulse" protocol diminished the ATP-induced Na^+ entry to 10 ± 7% (n = 11), compared to the standard protocol applied to the same cells. The inhibition of I_K under these conditions was only slightly reduced to 69 ± 20% (n = 11) of the inhibition observed under the standard protocol (Fig. 7 B). Obviously, in a given cell the inhibition of I_K does not directly correlate with the Na^+ entry through NSC channels. This suggests that I_K inhibition only requires local increases in $[Na^+]_i$ near the plasma membrane, which can be established almost independently of the overall Na^+ influx. The apparent contradiction between the results shown in Figs. 5 and 7 derives from the fact that Fig. 5 depicts cells with different densities of NSC channels and therefore different Na^+ influx. In contrast, Fig. 7 shows the reduction of charge entry at an almost constant density of activated NSC channels. Therefore, the density of open NSC channels within the membrane appears to be the most important parameter for I_K inhibition.

The dependence of I_K on $[Na^+]_i$ was also seen when PC-12 cells were dialyzed with pipette solutions containing Na^+ at concentrations varying between 20 and 120 mM (Fig. 8). The measured mean I_K density depended almost linearly on $[Na^+]_i$, with a 50% inhibition of I_K at about 60 mM. The typical I-V relation of inhibited I_K, characterized by a negative slope at positive potentials, was also seen during direct intracellular application of Na^+ (see Fig. 9 B).

Dialysis of cells with the various Na^+ concentrations caused a displacement of intracellular K^+ by Na^+, thereby reducing the concentration of the permeating ion species. The GHK equation (dashed line in Fig. 8) provides a prediction of the resulting inhibition of I_K. Although most of the observed I_K decrease can be attributed to the change of $[K^+]_i$, Fig. 8 may suggest that there is a further component of I_K inhibition. In the same line the significantly smaller I_K inhibition by extracellular NH_4^+ than by Na^+ (Fig. 4) hints

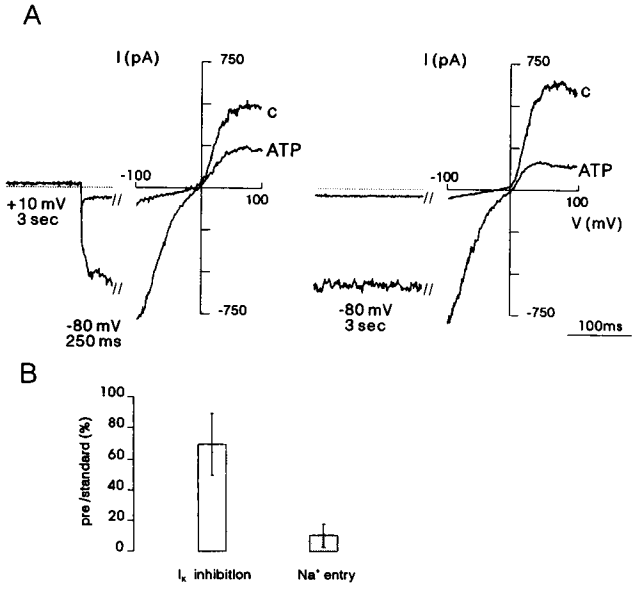

FIGURE 7 Modulation of macroscopic Na^+ entry and I_K inhibition by different voltage protocols. Two different voltage clamp protocols allowing a different Na^+ influx were compared on individual cells, and both protocols were repeated until steady-state I_K inhibition was reached. Control traces (c) and traces with steady-state inhibition of I_K in the presence of 20 μM ATP (ATP) are shown. (*A, left*) From a holding potential of 10 mV, 200-ms voltage ramp pulses from −100 to 100 mV, preceded by 250-ms prepulses to −80 mV, were applied at 0.33 Hz (prepulse protocol). In the presence of ATP, an inward current was elicited only during the prepulse and the negative part of the ramp pulses. (*Right*) Inhibition of I_K was measured with the standard protocol (holding potential −80 mV) (both panels from cell c2706ai). (*B*) The bars represent the relative inhibition of I_K and the Na^+ influx observed with the prepulse protocol (holding potential 10 or 30 mV, n = 11) normalized to the values obtained with the standard protocol from the same cells. The Na^+ influx was approximated from the start of ATP application until steady-state inhibition of I_K. Integral inward fluxes at −80 mV and during the voltage ramps were considered with 90%. The error due to outward I_K was neglected (<2%). Fluxes at 10 or 30 mV were determined from the respective prepulse amplitude according to Eq. 5. I_K inhibition was measured at 80 mV.

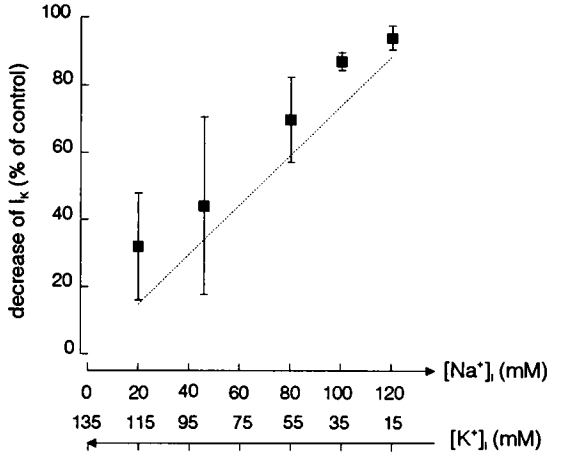

FIGURE 8 Effect of Na^+ infusion on I_K density in PC-12 cells. The cells were dialyzed with different Na^+ containing internal solutions (see Materials and Methods). The infused Na^+ concentrations are given on the abscissa. The filled squares illustrate the relative decrease of I_K after infusion of Na^+ ($n \geq 5$ for each concentration). The values express the decrease of the I_K density (±SD) with respect to the mean control I_K density at 80 mV ($n \geq 5$) measured with the Na^+-free standard internal solution from the same experimental series. The dashed line shows the relative decrease of I_K at 80 mV due to the change of $[K^+]_i$. The curve was calculated using the GHK current equation: $I_K/I_{K,con} = ([K^+]_i - a * [K^+]_o)/([K^+]_{i,con} - a * [K^+]_o$; with $[K^+]_o$ = 5.4 mM; $[K^+]_{i,con}$ = 135 mM; T = 37°C; a = $\exp(-FE/RT)$. $[K^+]_o$, extracellular K^+ concentration. The index (con) denotes the standard conditions, and $I_{K,con}$ was normalized to 100%.

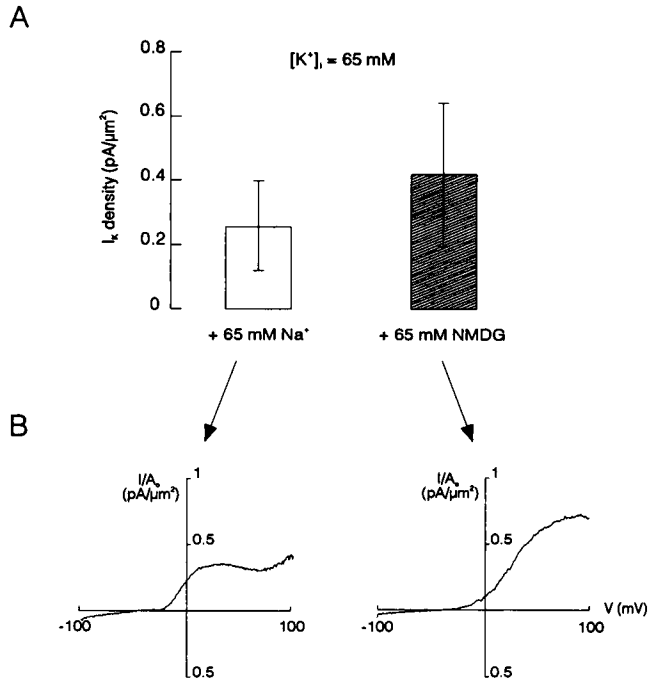

FIGURE 9 Specific I_K alteration by intracellular Na^+. (*A*) The I_K densities were measured from cells infused with 65 mM K^+ supplemented with either 65 mM Na^+ ($n = 14$) or NMDG ($n = 12$) (see Materials and Methods). The mean I_K densities ± SDs are shown. The values are significantly different ($p < 0.05$, *t*-test). (*B*) The *I-V* curves of two characteristic cells after infusion of Na^+ (*left*) or NMDG (*right*) are illustrated (cells c2605cf and c2605da). Intracellular Na^+ but not NMDG changed the voltage dependence of I_K in the same manner as activation of Na^+ influx by ATP. Currents were stimulated using the standard voltage ramp protocol.

at an additional Na^+-specific mechanism of K^+ channel blockage. Therefore, we measured I_K with a pipette solution containing 65 mM K^+ supplemented with either 65 mM Na^+ or the nonalkali cation NMDG. Na^+ in the pipette significantly reduced I_K density in comparison to NMDG (Fig. 9 *A*). Furthermore, only Na^+ but not NMDG induced a negative conductance region on the *I-V* relation of I_K (Fig. 9 *B*).

DISCUSSION

It is generally accepted that all known NSC channels mediate Na^+ entry into the cell. However, the consequences of Na^+ influx, which largely depend on the intracellular distribution and accumulation of Na^+, have not been thoroughly investigated.

Our experiments show that Na^+ influx through I_{ATP} induces a strong suppression of the outward I_K in PC-12 cells. Similar Na^+-dependent effects were observed upon nAChR activation in differentiated PC-12 cells (data not shown), suggesting a common mechanism for different NSC channels.

Most probably the entry and subsequent accumulation of Na^+ in the cells leads to a displacement of intracellular K^+, thereby reducing the electrochemical gradient for outward I_K. An additional Na^+-specific I_K inhibition is indicated by the significant reduction of I_K density by substitution of intracellular NMDG with Na^+. Infusion of Na^+ as well as ATP-induced Na^+ entry induced a characteristic *I-V* relation of I_K with a negative slope at positive potentials. A similar voltage-dependent inhibition of K^+ channels by intracellular Na^+ was previously observed (French and Shoukimas, 1985; Horie et al., 1987) and attributed to the binding of Na^+ at the inner K^+ channel pore. An inhibition by intracellular Na^+ was also confirmed for the outward rectifying DRK1 channel expressed in PC-12 cells (Sharma et al., 1993; Lopatin and Nichols, 1994).

Preliminary experiments on inside-out patches revealed a variable but clear decrease of single K^+ channel amplitudes in PC-12 cells when 50 mM Na-aspartate was applied to the intracellular face of the membrane.

The inhibition of I_K, measured with the standard protocol, was exponentially related to the amount of entering Na^+ ions. However, in individual cells, reduction of Na^+ entry by an alternative voltage protocol did not efficiently change I_K inhibition. Hence, the cell-specific spatial density of opened NSC channels and not the total amount of Na^+ entry is crucial for suppression of I_K. We conclude that a local Na^+ accumulation near the plasma membrane is responsible for the inhibition of I_K. In such a quasi "two-dimensional" situation, illustrated in Fig. 10, concentration changes are almost independent of the number of entering ions but more sensitive to the number of influx sources, i.e., the density of I_{ATP}. Hence, even small amounts of entering Na^+ ions may suppress I_K under depolarizing physiological conditions.

Discrete local concentration changes have already been shown for Ca^{2+} entry through voltage-dependent Ca^{2+} channels, leading to the proposal of different Ca^{2+} domain

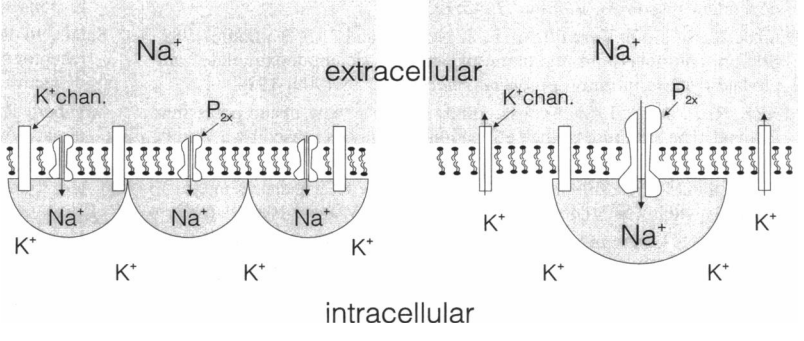

FIGURE 10 Geometrical model of Na^+ accumulation near the plasma membrane and its dependence on the spatial NSC channel (P_{2x} receptor) density. The model illustrates the distribution of Na^+ near the plasma membrane considering only a homogeneous diffusion of Na^+ from the activated NSC channels. The influx of equal amounts of Na^+/membrane area (represented by the *gray half-circles*, having equal total volumes if considered as half-spheres) is shown at a high (*left*) and a low (*right*) spatial density of NSC channels. Only in the case of one Na^+ influx source (*right*) is K^+ available close to the plasma membrane, allowing outward I_K.

models. These models assume a layer of Ca^{2+} accumulation under the plasma membrane ("macrodomain"; Chad and Eckert, 1984), or $[Ca^{2+}]_i$ rises directly at the inner mouth of the Ca^{2+} channel ("microdomain"; Llinás et al., 1991). The delay between Na^+ entry and I_K inhibition observed in our experiments suggests that Na^+ accumulation occurs in a finite layer similar to the "macrodomain" for Ca^{2+} accumulation (Chad and Eckert, 1984). In the cell shown in Fig. 6 *A* (membrane capacitance (C_m) = 6 pF, volume ≈ 1.4 pl, assuming spherical geometry and a specific capacitance of 1 $\mu F/cm^2$) an integral Na^+ influx of 470 pC, as measured with the prepulse protocol, would increase the total $[Na^+]_i$ only to less than 4 mM, even neglecting the possible active Na^+ extrusion. Because the observed I_K inhibition requires an elevation of $[Na^+]_i$ to more than 60 mM, the shell of Na^+ accumulation may be not thicker than 140 nm.

The local accumulation of Na^+ may also occur under physiological conditions when the cation influx is reduced by membrane depolarization. This would explain the fact that I_K blockage by tetraethylammonium only slightly modulates ATP-induced neurotransmitter secretion in PC-12 cells (Nakazawa and Inoue, 1992). Thus, even a small Na^+ influx through NSC channels possibly regulates the activity of other Na^+-dependent enzymes (Dumas et al., 1989), transporters (Attwell et al., 1993), or ion channels (Kawahara et al., 1990), serving as an additional signal transduction mechanism coupled to NSC channel activation.

We are grateful to Mrs. I. Reinsch for expert technical assistance and Mr. W. Stamm for skillful engineering. We also thank Dr. A. Lückhoff for helpfull discussions and Mrs. A. Hembold and Dr. I. F. Musgrave for carefully reading the manuscript.

REFERENCES

Attwell, D., B. Barbour, and M. Szatkowski. 1993. Nonvesicular release of neurotransmitter. *Neuron.* 11:401–407.

Benham, C. D., and R. W. Tsien. 1987. A novel receptor-operated Ca^{2+}-permeable channel activated by ATP in smooth muscle. *Nature.* 328: 275–278.

Borges, K., C. Ohlemeyer, J. Trotter, and H. Kettenmann. 1994. AMPA/kainate receptor activation in murine oligodendrocyte precursor cells leads to activation of a cation conductance, calcium influx and blockade of delayed rectifying K^+ channels. *Neuroscience.* 63:135–149.

Brake, A. J., M. J. Wagenbach, and D. Julius. 1994. New structural motif for ligand-gated ion channels defined by an ionotropic ATP receptor. *Nature.* 371:519–523.

Chad, J. E., and R. Eckert. 1984. Calcium domains associated with individual channels can account for anomalous voltage relations of Ca^{2+}-dependent responses. *Biophys. J.* 45:993–999.

Dumas, R. S., R. Z. Terwilliger, E. J. Nestler, and J. F. Tallman. 1989. Sodium and potassium regulation of guanine nucleotide-stimulated adenylate cyclase in brain. *Biochem. Pharmacol.* 38:1909–1914.

French, R. J., and J. J. Shoukimas. 1985. An ion's view of the potassium channel. The structure of the permeation pathway as sensed by a variety of blocking ions. *J. Gen. Physiol.* 85:669–698.

Gola, M., and M. Crest. 1993. Colocalization of active KCa channels and Ca^{2+} channels within Ca^{2+} domains in Helix neurons. *Neuron.* 10:689–699.

Gollasch, M., J. Hescheler, K. Spicher, F.-J. Klinz, G. Schultz, and W. Rosenthal. 1991. Inhibition of Ca^{2+} channels via α_2-adrenergic and muscarinergic receptors in pheochomocytoma (PC-12) cells. *Am. J. Physiol.* 260:C1282–C1289.

Hagiwara, S., and K. Takahashi. 1974. The anomalous rectification and cation selectivity of the membrane of a starfish egg cell. *J. Membr. Biol.* 18:61–80.

Hamill, O. P., A. Marty, E. Neher, B. Sakmann, and F. J. Sigworth. 1981. Improved patch-clamp techniques for high-resolution current recordings from cells and cell-free membrane patches. *Pflügers Arch.* 391:85–100.

Hescheler, J., and G. Schultz. 1993. Nonselective cation channels: physiological and pharmacological modulations of channel activity. *In* Nonselctive Cation Channels: Pharmacology, Physiology and Biophysics. D. Siemen and J. Hescheler, editors. Birkhäuser, Basel. 27–43.

Hille, B., and W. Schwarz. 1978. Potassium channels as multi-ion single-file pores. *J. Gen. Physiol.* 72:409–442.

Hodgkin, A. L. 1951. The ionic basis of electrical activity in nerve and muscle. *Biol. Rev.* 26:339–409.

Horie, M., H. Irisawa, and A. Noma. 1987. Voltage-dependent magnesium block of adenosine-triphosphate-sensitive potassium channel in guinea-pig ventricular cells. *J. Physiol.* 387:251–272.

Hoshi, T., and R. W. Aldrich. 1988a. Voltage-dependent K^+ currents and underlying single K^+ channels in pheochromocytoma cells. *J. Gen. Physiol.* 91:73–106.

Hoshi, T., and R. W. Aldrich. 1988b. Gating kinetics of four classes of voltage-dependent K^+ channels in pheochromocytoma cells. *J. Gen. Physiol.* 91:107–131.

Imredy, J. P., and D. T. Yue. 1992. Submicroscopic Ca^{2+} diffusion mediates inhibitory coupling between individual Ca^{2+} channels. *Neuron.* 9:197–207.

Inoue, K., K. Nakazawa, K. Fujimori, and A. Takanaka. 1989. Extracellular adenosine 5′-triphosphate-evoked norepinephrine secretion not relating to voltage-gated Ca channels in pheochromocytoma PC12 cells. *Neurosci. Lett.* 106:294–299.

Jabs, R., F. Kirchhoff, H. Kettenmann, and C. Steinhauser. 1994. Kainate activates Ca^{2+}-permeable glutamate receptors and blocks voltage-gated K^+ currents in glial cells of mouse hippocampal slices. *Pflügers Arch.* 426:310–319.

Kawahara, K., M. Hunter, and G. Giebisch. 1990. Calcium-activated potassium channels in the luminal membrane of *Amphiuma* diluting segment: voltage-dependent block by intracellular Na^+ upon depolarisation. *Pflügers Arch.* 416:422–427.

Kim, W.-K., and R. Rabin. 1994. Characterisation of the purinergic P_2 receptors in PC12 cells. *J. Biol. Chem.* 269:6471–6477.

Llinás, R., I. Z. Steinberg, and K. Walton. 1991. Relationship between presynaptic calcium current and postsynaptic potential in squid giant synapse. *Biophys. J.* 33:323–352.

Lopatin, A. N., and C. G. Nichols. 1994. Internal Na^+ and Mg^{2+} blockade of DRK1 (Kv2.1) potassium channels expressed in *Xenopus* oocytes. *J. Gen. Physiol.* 103:203–216.

Nakazawa, K., K. Fujimori, A. Takanaka, and K. Inoue. 1990. An ATP-activated conductance in pheochromocytoma cells and its suppression by extracellular calcium. *J. Physiol.* 428:257–272.

Nakazawa, K., and P. Hess. 1993. Block by Ca^{2+} of ATP-activated channels in pheochromocytoma cells. *J. Gen. Physiol.* 101:377–392.

Nakazawa, K., and K. Inoue. 1992. Roles of Ca^{2+} influx through ATP-activated channels in catecholamine release from pheochromocytoma PC12 cells. *J. Neurophysiol.* 68:2026–2032.

Roche, E., and M. Prentki. 1994. Calcium regulation of immediate-early response genes. *Cell Calcium.* 16:331–338.

Sands, S. B., and M. E. Barish. 1992. Neuronal nicotinic acetylcholine receptor currents in phaeochromocytoma (PC12) cells: dual mechanisms of rectification. *J. Physiol.* 447:467–487.

Schubert, R. 1990. A program for calculating multiple metal-ligand solutions. *Comp. Methods Progr. Biomed.* 33:93–94.

Schulman, H. 1993. The multifunctional Ca^{2+}/calmodulin-dependent protein kinases. *Curr. Opin. Cell. Biol.* 5:247–253.

Sharma, N., G. D'Arcangelo, A. Kleinklaus, S. Halegoua, and J. S. Trimmer. 1993. Nerve growth factor regulates the abundance and distribution of K^+ channels in PC12 cells. *J. Cell Biol.* 123:1835–1843.